Journal of Environmental Management 317 (2022) 115431

Contents lists available at ScienceDirect

Journal of Environmental Management

journal homepage: www.elsevier.com/locate/jenvman

Research article

Mechanochemical debromination of waste printed circuit boards with marble sludge in a planetary ball milling process

Gerard Gandon-Ros [a,b], Ignacio Aracil [a,b], María Francisca Gómez-Rico [a,b], Juan A. Conesa [a,b,*]

[a] Institute of Chemical Process Engineering, University of Alicante, P.O. Box 99, E-03080, Alicante, Spain
[b] Department of Chemical Engineering, University of Alicante, P.O. Box 99, E-03080, Alicante, Spain

ARTICLE INFO

Keywords:
Mechanochemistry
Printed circuit boards
Flame retardants
Waste valorisation
Co-milling
TBBPA

ABSTRACT

An effective management of waste printed circuit board (WCB) recycling presents significant advantages of an economic, social, and environmental nature. This is particularly the case when a suitable valorisation is made of the non-metallic parts of the WCBs, well known for their "hidden" toxicological risks. Such benefits motivate research on techniques that could contribute to mitigating their adverse socio-environmental impacts. In this work, waste printed circuit boards (WCBs) containing tetrabromobisphenol A (TBBPA) as a brominated flame retardant (BFR) underwent debromination using a mechanochemical treatment (MCT) and marble sludge, another recoverable waste, as well as pure CaO as additives. All runs in this work were performed at an intermediate rotation speed of 450 rpm, using additive/WCB mass ratios (R_m) of 4:1 and 8:1, ball to powder ratios (BPR) of 20:1 and 50:1, treatment times from 2.5 h to 10 h, two WCB sizes (powder and 0.84 mm) and marble sludge, from original to precalcined conditioning. Stainless steel jars and balls were used to verify the effect of each parameter on the system and to seek an optimum process. Complete debromination of 0.84 mm WCBs was achieved at 450 rpm, using a R_m of 8:1, a BPR of 50:1, a residence time of 10 h (more than 95% in only 5 h), and a precalcined marble sludge as additive. The results revealed that when using a R_m of 4:1 instead of 8:1, more waste could be effectively treated, per batch with a lesser need for additives, at the expense of a slightly lower level of debromination efficiency. In the same way, an appropriate apparent ball diameter (with respect to the volume of the used jar) should be carefully studied in relation to WCB size in order to achieve a beneficial total amount of energy transfer during milling.

1. Introduction

In 2019, some 53.6 million metric tons (Mt) of waste electric and electronic equipment (WEEE), also called e-wastes, were generated worldwide. And that figure is forecast to reach 74.7 Mt by 2030. Specifically, e-waste includes WCBs, which contain several toxic additives, mainly BFRs, estimated to represent 71 kt per year in global undocumented flows (Forti et al., 2020). In addition, approximately 90% of WCBs ends up in landfills or is incinerated in Europe (Composite Recycling Ltd, 2017). The main BFRs used in WCBs are TBBPA and polybrominated diphenyl ethers (PBDEs), and the pollution caused by their presence is considerable. Indeed, the use of certain PBDEs such as decabromodiphenyl ether is no longer permitted in new electrical and electronic devices within the European Union since 2008, but they still persist in soils which need to be decontaminated (Yi et al., 2021). Of particular concern is the suitable treatment of these BFRs (Eskenazi et al., 2017; Song et al., 2019), together with that of other compounds such as Dichlorodiphenyltrichloroethane (DDT) and polychlorinated biphenyls (PCBs), all believed to be endocrine-disrupting chemicals (EDCs) in humans and animals. During thermal treatment, BFRs can release toxic compounds such as polybrominated dibenzo-p-dioxins/furans (PBDD/Fs) (Altarawneh and Dlugogorski,

Abbreviations: WCBs, waste printed circuit boards; DE, debromination efficiency; WEEE, waste electric and electronic equipment; BFRs, brominated flame retardants; TBBPA, tetrabromobisphenol A; PBDEs, polybrominated diphenyl ethers; DDT, Dichlorodiphenyltrichloroethane; PCBs, polychlorinated biphenyls; EDCs, endocrine-disrupting chemicals; POPs, persistent organic pollutants; PBDD/Fs, polybrominated dibenzo-p-dioxins/furans; MCT, mechanochemical treatment; MCD, mechanochemical debromination; R_m, additive/WCB mass ratio; BPR, ball to powder ratio; D_0, total transferred energy; ICP-MS, Inductively coupled plasma mass spectrometry; XRF, X-ray fluorescence; TG, thermogravimetry; DTG, Differential thermogravimetric analysis; FTIR, Fourier transform infrared spectroscopy.

* Corresponding author. Institute of Chemical Process Engineering, University of Alicante, P.O. Box 99, E-03080, Alicante, Spain.
E-mail address: ja.conesa@ua.es (J.A. Conesa).

https://doi.org/10.1016/j.jenvman.2022.115431
Received 4 April 2022; Received in revised form 25 May 2022; Accepted 26 May 2022
Available online 29 May 2022

2015), even under controlled conditions (Dangtungee et al., 2012). For this reason, efforts should be made to remove the bromine present in BFRs in advance to avoid the formation of brominated compounds during the treatment processes (Sakai et al., 2001).

Eliminating or minimising the use of solvents during a previous debromination process has implications from the perspective of green chemistry (Takacs, 2014). Moreover, the use of a non-solvent technique could be more environmentally friendly and more compatible with EU waste disposal regulations. Given current rates of water scarcity and consumption, even the use of water as a green solvent should be progressively reduced: two-thirds of the world's population may actually face water shortages by 2025 (Leguen, 2019).

Mechanochemistry is a branch of chemistry with multiple applications, including waste treatment, since it does not require heating. The technique generates negligible gas emissions, consumes less energy, emits less carbon dioxide, produces less waste, and usually prevents the formation and release of unintentional persistent organic pollutants (POPs). Mechanochemistry can also treat wastes containing halogenated POPs (Gilman, 1996; Guo et al., 2010). No large plants with complex facilities should be required, and their simple system designs should make them more easily acceptable by local residents (Guo et al., 2010). For these reasons, mechanochemical treatment is an up-and-coming WCB debromination technique that produces insignificant pollution levels and that presents an accomplishable future industrialisation.

Furthermore, calcium oxide is the main additive employed in mechanochemical dehalogenation treatments (Moreno et al., 2019; Tongamp et al., 2009; Zhang et al., 1999, 2001, 2012, 2013), due to its reduced financial cost and the high absorption performance of the HBr or Br^- generated during the mechanochemical process. CaO powder presents high surface energy and activity, acting as an electron donor (Cagnetta et al., 2017). This makes it effective at breaking bromine bonds in a reduction reaction, since the bromine atom has high electronegativity (Lei et al., 2018).

Most published works on mechanochemical debromination have focused on the treatment of pure halogenated compounds. Zhang et al. (2012) reached maximum debromination efficiency (DE) with 60.0% and 95.3% of soluble bromide using CaO and Fe + SiO_2 respectively, when treating pure TBBPA (after grinding for 6 h) via mechanochemical reaction at 550 rpm, weight ratio 10:1 and a balls to materials ratio of 30:1.

To the best of our knowledge, very few studies exist on the mechanochemical degradation of BFRs contained in WCBs. One exception is the work of Wang et al. (2020), who achieved greater printed circuit board debromination performance with PBDE as BFR when using CaO than when employing MgO or Fe + SiO_2, reaching a DE of 98.0% after milling for 24 h under 400 rpm, using a weight ratio of 2:1 and a balls to materials ratio of 9:1.

Milling time should be reduced to improve the feasibility of mechanochemical debromination (MCD) (Ren et al., 2015), while introducing, where possible, other wastes as additives for the dehalogenation. This would facilitate future industrialisation thanks to cost reductions and a lower environmental impact. As CaO can be obtained from $CaCO_3$ through calcination, all $CaCO_3$-based waste, which is usually not very exploitable, could be useful too. In this way, Baláž et al. (2014) showed how using eggshell waste as a source of $CaCO_3$ could greatly improve the feasibility of the mechanochemical treatment of PVC, reaching a dechlorination efficiency of 95% after 4 h at 550 rpm, a molar ratio between Ca and Cl of 5.06:1 and a ball to powder ratio of 65:1.

Among the wastes used as additives, sludge is a great resource, either to pre-treat e-waste or to apply directly as an inhibitor agent in the formation of POPs during the incineration of PVC. This leads to a win-win combination, as proven by Gandon-Ros et al. (2021a) with sewage sludge.

The main objective of this work was to achieve a complete removal of bromine from WCBs containing TBBPA as BFR by MCD, using another waste as a co-grinding agent and minimising ball mill residence time. The waste added as a $CaCO_3$ source was marble sludge, whose reusability is limited. Different bromine removal conditions were compared, seeking the optimal parameters that could minimise the variable cost of the process and that would make it easier for MCD to compete with other techniques.

2. Materials and methods

2.1. Materials

The WCBs used were metal-free FR-4 epoxy fiberglass substrates supplied by CISA (Circuitos Impresos S.A., Spain). This WCB was 1 mm thick and consisted of an overlapping of 5 laminates of cross-linked glass fibre immersed in epoxy resin with flame retardant. The BFR employed was confirmed by Raman spectroscopy as TBBPA in previous studies (Gandon-Ros et al., 2021b; Soler et al., 2017). WCBs were cut into pieces using pliers, then ground with a Retsch SM 200 cutting mill and screened to a 0.84 mm × 0.84 mm particle size. Passed the screening, they were then milled with a vibratory disc mill Retsch RS 200 in cryogenic mode to obtain a fine powder particle size. A characterisation of WCBs with a 0.84 mm × 0.84 mm particle size was previously performed (Soler et al., 2017) by elemental analysis (27.5 wt% C, 2.5 wt% H, 1.1 wt% N and 24.6 wt% O), ash content (44.3 wt%) and bromine content determination (4.0 wt%). The fine WCB powder used here came from a recently received batch of WCBs from the same supplier with a 6.4% Br content. It was averaged after determination by oxygen combustion bomb-ion chromatography (Dionex DX-500) using four replicates and via Inductively Coupled Plasma Mass Spectrometry (ICP-MS) (Agilent 7700x) using two replicates, with a deviation between techniques of 2.9%. Both WCB sizes employed were obtained by crushing processes outside the ball milling process under study due to the ball mill feed size limitation (10 mm) and to avoid the undesirable reactions that would probably have been caused by long ball milling crushing runs.

The Marble sludge was provided by Mármoles Hermanos Jiménez (Alicante, Spain). After drying at 100 °C for 12 h, several analyses were launched to characterise the waste in its original version (MS) and its calcinated version (MS 800) for 2 h at 800 °C: elemental analysis, X-ray fluorescence (XRF), ICP-MS, Raman Spectroscopy and thermogravimetry (TG). In fact, calcination is usually employed to liberate CO_2 from materials that contain the calcite mineral (the most stable polymorph form of $CaCO_3$), such as limestone or seashells, and to produce CaO (the main additive employed in mechanochemical dehalogenation treatments). The elemental analyser Thermo Finnigan Flash 1112 provided a 15.46 and a 12.33 wt% C content for MS and MS 800, respectively, the rest corresponding to the ash content (also verified by calcinating 6 samples at 550 °C following the UNE-EN-14775:2009 (ECS Solid Biofuels - Determination of Ash Content, 2010), with a deviation between techniques of 0.4%). The XRF results (obtained using a Philips Magix Pro PW2400 equipped with a rhodium tube and beryllium window) and ICP-MS showed high Ca and Mg concentrations, which increased, as expected, after calcination (see Table S1 of the supplementary material). Raman and TG results, obtained using a microscopic confocal Raman spectroscope (LabRam, Jobin-Ivon) with an Argon laser at 514 nm and a TG analyzer (Mettler Toledo TGA/SDTA851e/SF/1100), are shown in section 3 below.

A quality grade CaO with a minimum purity of 96% (Sigma-Aldrich, Germany) was heated at 800 °C for 2 h to ensure its purity. This calcinated CaO (CaO 800) was then used as a reference to compare most of the experiments performed. Every additive employed in this work was in fine powder.

Finally, the particle size distribution of all the raw materials used in this study, except for the 0.84 × 0.84 mm WCB sample, were also determined via wet laser diffraction with an MICROTRAC SYNC (VERDER SCIENTIFIC). Even after having been screened to a size of 0.84 × 0.84 mm, the highly elongated shape of most WCB sample

particles caused one of the dimensions to exceed the particle size limit permitted to use the analysis equipment (2 mm). The CaO particle size distribution curves (obtained assuming the sample as calcium oxide particles with IR = 1.83), MS (obtained assuming the sample as calcium carbonate particles with IR = 1.49), MS 800 (obtained assuming the sample as calcium carbonate particles with IR = 1.49) and WCB powder (obtained assuming the sample as silicon dioxide particles with IR = 1.51), are presented in figures S1A, S2A, S3A and S4A. In the same way, using a high-speed camera, a series of photographic captures were taken of each individual particle included in the analysed samples, showing the largest and smallest particles, as shown in figures S1B, S2B, S3B, S4B, and S1C, S2C, S3C, S4C, respectively.

2.2. Planetary ball mill for mechanochemical debromination

All debromination runs were conducted using an air atmosphere at 450 rpm in two 50 mL stainless steel jars with 7 stainless steel 15 mm-diameter balls per jar (as recommended by the manufacturer) inside the reactor (95.3 g total ball weight), using several additives as CaO 800, MS and MS 800, and two WCB sizes. The planetary ball milling Retsch PM100 employed was supplied by Biometa S.A (Spain). This "mechanochemical reactor" is able to resist a sun wheel speed of 650 rpm, grinding up to 33.3 times the acceleration of gravity (G-force), which corresponds, according to a 1:-2 speed ratio, to a jar speed of 1300 rpm in the opposite direction of the sun wheel rotation.

Every run was operated under an automated change of rotation direction every 15 min, including a 1 min pause between each direction change to avoid a temperature excess inside the jars and hence, unwanted secondary degradation reactions. In addition, the accumulation or agglomeration of ground material was prevented at certain points in the jar during the milling. Moreover, the debromination process was managed by varying the additive/WCB mass ratio (R_m), the ball to powder (WCB + additive) ratio (BPR), the residence time, the WCB size and the type of additive.

In addition, to conduct the debromination process, the milling intensity (I) was defined as the rate of energy transfer to milled powder (the powder refers to the sum of the WCB and the reagent):

$$I = \frac{1}{2} m_b v_i^2 NF \tag{1}$$

That is, the milling intensity is the kinetic energy ($1/2 \cdot m_b v_i^2$, being v_i their velocity) delivered to the powder through the N balls (each of mass m_b) through F hits per time unit. In the present work, all runs were performed using the same rotational speed and number of balls, in such a way that the v_i and F values would be constant across the runs. Based on the calculations of Concas et al. (2006), average ball velocity could be considered close to v_i = 4.169 m/s, the impact frequency being F = 142.04 Hz, so the impact intensity was 117.6 W, equivalent to 1234 W/g of balls.

2.3. Runs and conditions

2.3.1. Debromination in planetary ball mill

A total of 36 debromination experiments were conducted at 450 rpm (an upper mid-range rotation speed) with an R_m of 4:1 or 8:1, a BPR of 20:1 or 50:1, treatment times from 2.5 h to 10 h, WCB sizes from powder to 0.84 mm, and marble sludge, from its original state to precalcined conditioning (in addition to the use of precalcined CaO as a reference additive), as shown in Table S1. An experimental error below 3.9% was calculated based on replicate experiments.

During the debromination process, solid phase reactions were being produced. Bromine diffusion and reaction with the CaO or marble sludge were the main mechanisms implied, producing different brominated inorganic materials such as $CaBr_2$, $Ca(BrO_3)_2$ and/or $Ca(BrO_2)_2$. After milling for 2.5, 5 and 10 h, a minimal part of the sample was extracted from each jar to determine the inorganic bromine content in order to keep any alterations to the reaction medium in progress to a minimum. This point was carefully considered in this work due to the high R_m and BPR ratios used. Therefore, it was preestablished that at no time should the sum of these exceed 15% of the initial mass of the jar sample extractions during the 10 h duration of the experiment. It was thus essential to quantify the amount of extracted sample required for a minimal interference in the debromination reaction. Indeed, the concentration would indirectly increase due to the reduction of the mass sample inside the reaction chamber over time, causing concentration measurement errors that would need to be corrected. For this, the evolution of the debromination efficiencies (DE) over time was determined as if they were reached for each condition in an identical process with no extractions (Gandon-Ros et al., 2020). Based on this correction, the corresponding bromine mass $m_{Br,t}$ (in mg) remaining inside the reaction chamber at any time t (in hours) was calculated as follows:

$$m_{Br,\,t}(t=0) = [Br]_{t=0} \cdot m_{sample} \tag{2}$$

$$m_{Br,\,t}(\forall_{t>0}) = [Br]_t \cdot \left(m_{sample} - \sum_{t=1}^{t} m_{Ext_{t-1}} \right) \tag{3}$$

here, $[Br]_t$, the bromine concentration in the aqueous dilution was obtained by dissolving each sample extraction at any time t (in mg/kg); m_{Sample} was the sample weight initially introduced inside the reaction chamber (in kg) that would remain the same until the end of the reaction in a process without extractions; and $m_{Ext,t-1}$ was the sample weight (in kg) extracted at any time t-1 (in hours).

DE represents the amount of organic bromine content that was completely removed from the solid and transferred to the aqueous phase as soluble bromine (thus achieving an easily washable residue by aqueous rinsing) at any time t, and was calculated as:

$$DE_t(\%) = \frac{m_{Br,t}}{m_{Br,\,i}} \tag{4}$$

where $m_{Br,i}$ was the initial weight of bromine content in WCBs inside the reactor chamber and $m_{Br,t}$ was the weight of bromine at any time t inside the reaction chamber considering the correction explained previously.

One portion of 0.10 and 0.15 g of each milled extracted sample was solved each time in 25 mL of ultra-pure water for experiments with a R_m of 4:1 and 8:1, respectively. An ultrasonic treatment was performed for 30 min followed by an automated oscillator-vibratory stirring that was conducted at around 500 rpm for 30 min to ensure the complete dissolution of any remaining soluble bromide. After appropriate dilution and filtration, each sample was analysed via ion chromatography (IC) (Metrohm, 850 ProfIC AnCat- MCS) to determine the soluble bromide content.

At the end of the MCD, the remaining sample was collected once the jar cooled down to room temperature. It was then analysed by Fourier-transform infrared spectroscopy (FTIR) (BRUKER IFS 66/S with ATR Specac Golden Gate prism, Germany) applying the attenuated total reflection method (ATR Golden gate mode) from 500 cm^{-1} to 4000 cm^{-1} so as to corroborate, at least qualitatively, the effective destruction of TBBPA and thus support the results obtained by IC for DE.

2.3.2. Analysis of the preconditioning effect of debromination agents and WCBs on MCD

The debromination additives were analysed in order to find which properties and/or characteristics could improve the debromination efficiencies. These improvements made thanks to the precalcination treatment are presented later, in the discussion of the results. The additives (CaO 800, MS and MS 800) were analysed by Raman spectroscopy and by TG. TG runs were conducted employing 8 mg of sample under combustion and pyrolysis conditions at a flow rate of 100 mL min^{-1} and a heating rate of 5 °C min^{-1} up to 850 °C, along with a differential thermogravimetric (DTG) representation to facilitate the detection of small-scale changes in TGs.

Additionally, an empirically-based comparative model was applied to better understand, using a simple numerical calculation, the extent to which the global potential of the process was being exploited when seeking to correctly adapt the WCB size to a "diameter balls/jar volume" set. To do so, new terms such as Total Surface of Contact (TSC) and Impact on Debromination due to Sample Size (IDESS) are presented in section 3 of the manuscript.

3. Results and discussion

3.1. WCB debromination and optimal MCD parameters when using CaO and marble sludge

The breaking, impact and flattening actions experienced by WCBs ground by ball milling provoke the resin matrix and BFRs inside into taking part in physical-chemical reactions, making the degradation process more complicated than the reported pure state (Huang et al., 2016). In this way, it is likely that the debromination would require more severe reaction conditions, in addition to possibly long reaction times, as reported by Wang et al. (2020). In this latter study, a quasi-complete debromination of a WCB containing PBDE as BFR was achieved after 24 h milling under 400 rpm, a weight ratio of 2:1, and a balls to materials ratio of 9:1. According to Schmidt et al. (2016), the higher the BPR ratio, the higher the temperature reached and the DE that could be achieved. The temperature may also influence the degradation rate and the C–Cl bond breaking process, which is endothermic (Dong et al., 2019). According to Cagnetta et al. (2016), chlorinated and brominated compounds have a chemical structure and relative bond weakness similar to that of the aromatic carbon-halogen bond (C–Cl with 407 kJ/mol, C–Br with 346 kJ/mol). They hence share similar fates during the MC treatment. That is why higher BPR and R_m ratios were used in this work to achieve a complete debromination in less time. Marble sludge is mainly composed by Ca (see Table S2), responsible for capturing Br ions during ball milling and forming the inorganic salt $CaBr_2$ or its hydrated form (Wang et al., 2020).

Fig. 1A shows that the DE evolution over time of the sample MS 800 at BPR 50:1 could be assimilated to the evolution of the sample CaO 800 at BPR 20:1 when using a R_m of 4:1. Thus, the fact that MS 800 at BPR 50:1 had less Ca content than CaO 800 at BPR 20:1 was compensated by the lower amount of waste to treat in the first case for a given ball weight (see Table S2). Moreover, each DE obtained after 10 h showed a difference of around 20% when comparing both additives at BPR 50:1. Considering that marble sludge was a low-value waste and CaO was a high-level grade additive, a 20% difference of DE after 10 h is highly positive. In this work, no direct comparisons were made with other authors regarding the use of CaO for a number of reasons. First, although WCB was also treated in Wang et al. (2020), the BFR inside was PBDE and not TBBPA. For their part, Zhang et al. (2012) worked with TBBPA

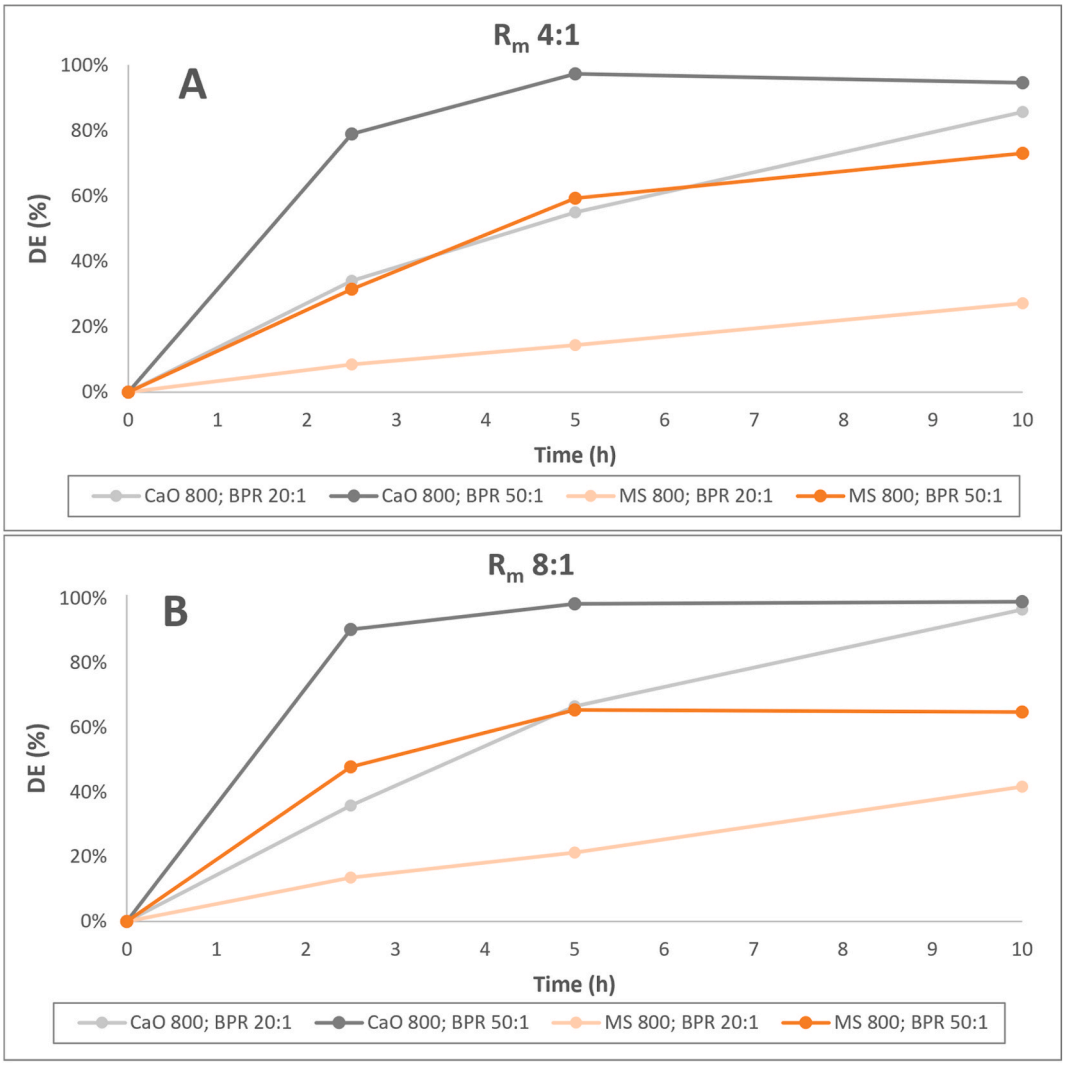

Fig. 1. Evolution and global behaviour of DE obtained at 450 RPM when debrominating WCB powder with both precalcined additives employed in this work, keeping R_m at 4:1 (Fig. 1A) and 8:1 (Fig. 1B).

as a pure compound. Second, the parameter difference was remarkable, working at 450 rpm in the present study instead of 400 or 550 rpm in the study of Wang et al. (2020) and Zhang et al. (2012), respectively. In addition, the R_m and BPR parameters used in this work were completely different from that of those studies, where R_m 2:1 and BPR 9:1 (Wang et al., 2020) and R_m 11:1 and BPR 30:1 (Zhang et al., 2012) were applied, respectively. Fig. 1B shows a similar evolution between both additives when using R_m 8:1, but a larger gap appears between the curves after 10 h. In fact a higher R_m of 8:1 appeared to be beneficial (+20% increase in DE) only for CaO 800 and MS 800 when a low BPR 20:1 was used, as visible in the comparison of the final results in Fig. 1A and B. When seeking to achieve a complete or quasi-complete debromination, based on Fig. 1, where possible, the use of a R_m of 4:1 would be more suitable because less additive would be needed and more waste per run could be treated.

Fig. 2 shows that DE evolution over time was only slightly affected by a changing R_m. Indeed, the gain with both calcined additives, comparing 8:1 to 4:1, was irrelevant when working with a BPR of 20:1 (Figs. 2A) and 50:1 (Fig. 2B), respectively. In addition, for each run using a BPR of 50:1, an asymptote always seemed to be attained much more rapidly (also doubling the final performance achieved when MS 800 was used with respect to the BPR of 20:1). The latter supports the fact that the optimum process seemed to be a BPR of 50:1 and a R_m of 4:1. To avoid being limited by the apparent asymptote that could be reached for BPR 50:1 and R_m 4:1, even using MS 800, a lower BPR or R_m should be studied to better optimise the time needed for a complete WCB debromination (in this way, a greater amount of WCBs could even be treated in each run).

Fig. 3A shows an example of several replicates revealing a strong similarity with an average experimental error below 3.9%. The reason for calcinating the marble sludge was to obtain a rapid debromination rate increase. However, that seemed to be more a constraint as of a 10 h duration of reaction, as the evolution followed was comparable to an asymptote, unlike the use of original marble sludge that seemed to keep increasing linearly. Following these results, further detailed and relevant information is shown in section 3.2.

Fig. 3B shows the results obtained with WCB size increases. The benefit of the previous marble sludge calcination became apparent, since by increasing the WCB size, a DE of 80% was obtained in only 2.5 h. It was in fact already over 95% after only the first 5 h and 100% after 10 h. Based on Figs. 1 and 2, even better results could have been expected if Fig. 3 experiments had been conducted with BPR 50.1 and R_m 4:1.

Since the WCB size cannot really be much larger for the mill to work properly (<3–4 mm in a 50 mL jar when using 15 mm diameter balls), the most appropriate decision would probably be to reduce the size of the balls to improve the total transferred energy (D_0) and therefore the final DE (Chen et al., 2017).

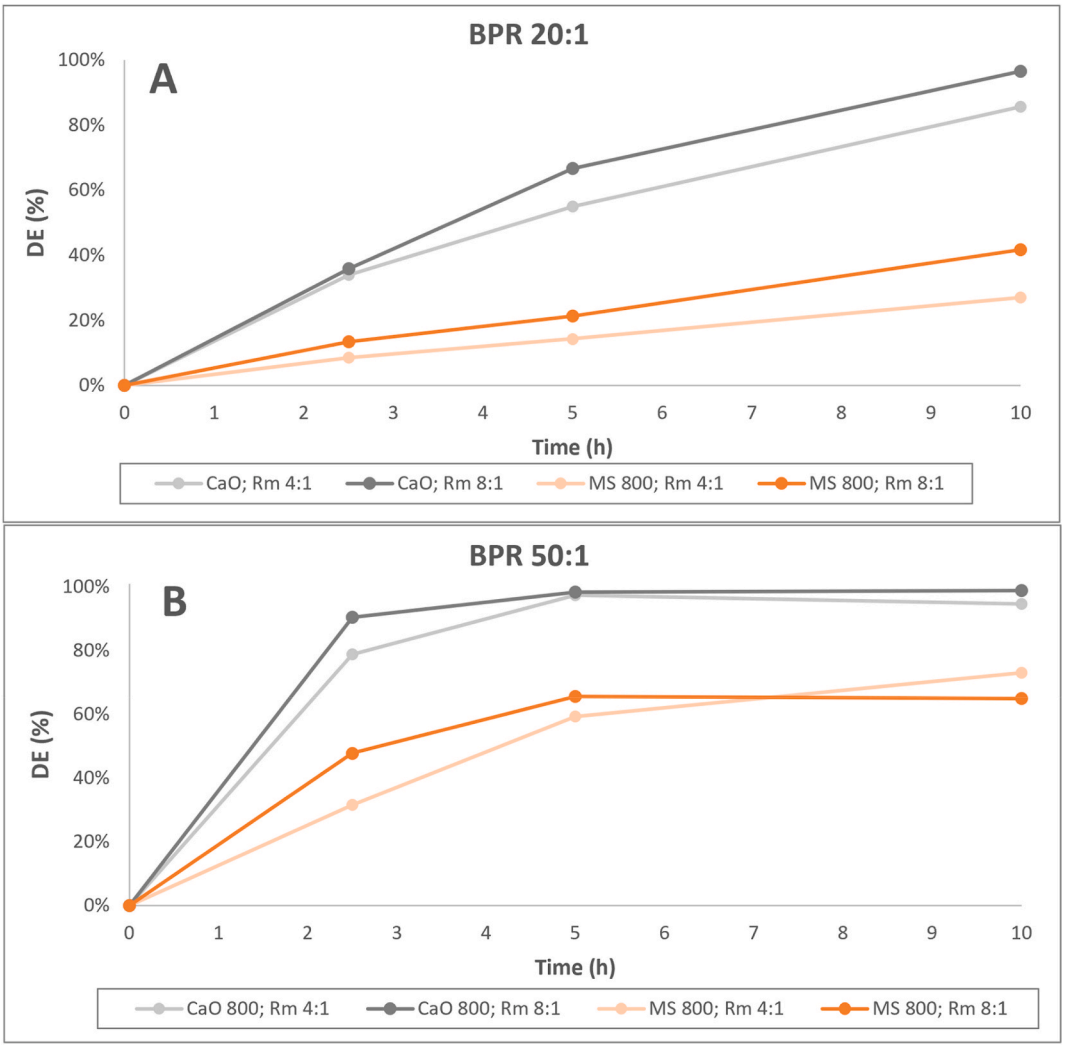

Fig. 2. Evolution and global behaviour of DE obtained at 450 RPM when debrominating WCB powder with both precalcined additives employed in this work, keeping the BPR at 20:1 (Fig. 2A) and 50:1 (Fig. 2B).

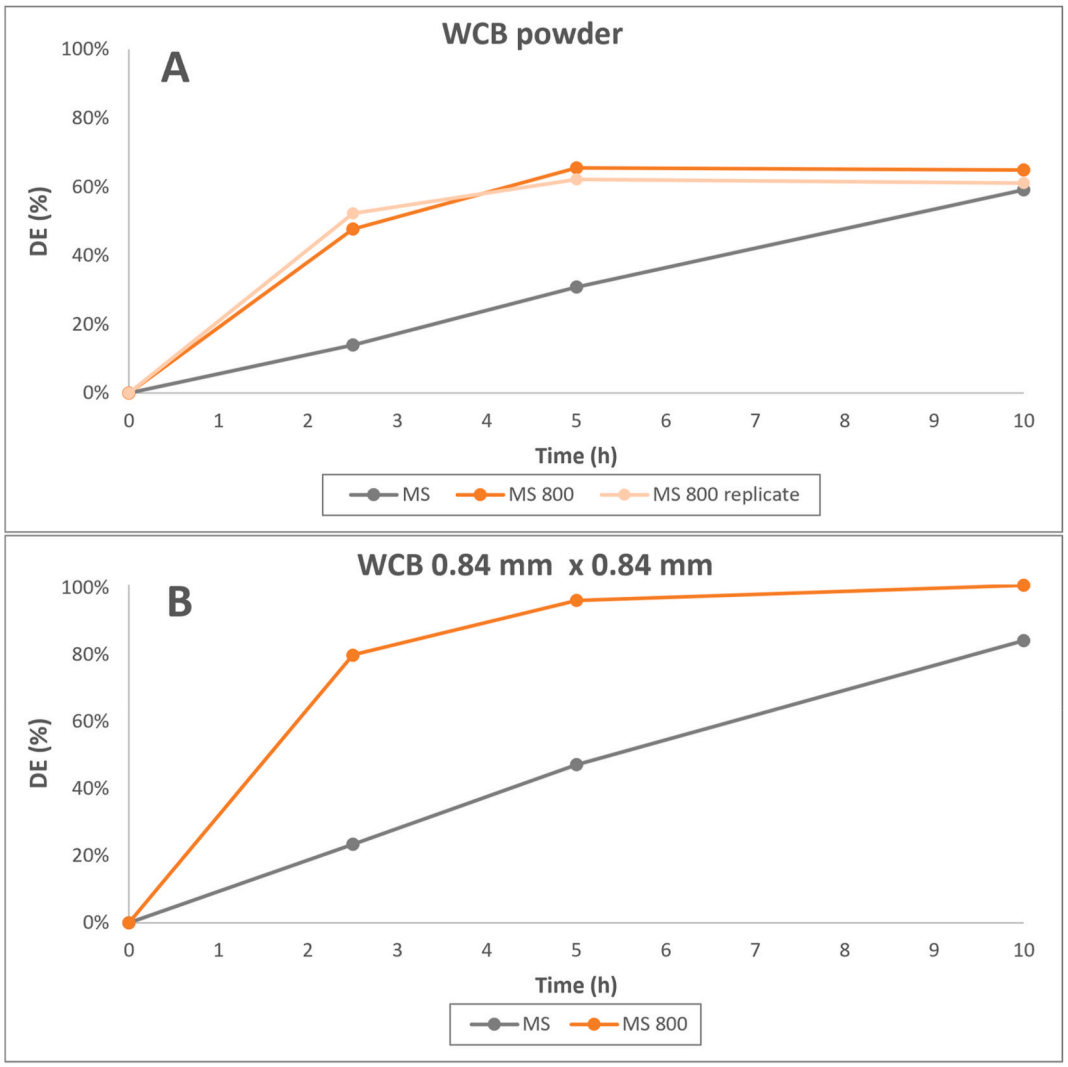

Fig. 3. Evolution and global behaviour of DE obtained at 450 RPM when debrominating WCB powder (Fig. 3A) and 0.84 mm × 0.84 mm sized WCB (Fig. 3B) with both versions of marble sludge employed in this work, BPR 50:1 and R_m 8.1.

In a case such as this, it would have been interesting to observe the evolution of the particle size distributions of all the solid residues according to grinding time (over 2.5, 5 and 10 h). Only the final ones (10 h) were collected since the minimum possible sample was extracted at all times to avoid interactions with the ongoing reaction medium due to the high BPR and Rm conditions.

Therefore, the particle size distribution of only one of the final residues was analysed as an example, more specifically, the solid residue of experiment 35 (see Table S1), for which complete debromination was achieved. Fig. S5A shows the particle size distribution curve of the solid residue at the end of experiment 35 (obtained assuming the sample as $CaBr_2$ absorbing particles, since the refractive index was not available in the equipment literature). In the same way, using a high-speed camera, a series of photographic captures was made of each individual particle making up the final solid residue analysed in experiment 35, showing those with the largest and smallest particle size, as shown in Figs. S5B, and S5C, respectively.

Fig. 4 represents the results of the FTIR analyses that were conducted on all the solid residues obtained after 10 h of MCD in order to confirm, at least qualitatively, the destruction of TBBPA. The analyses focused on the peak band around 700 cm^{-1} of the entire spectra (710 cm^{-1} in Fig. 4), which corresponded to the C–Br stretching vibration of the TBBPA molecule (Zhang et al., 2012) and was therefore directly related to the release of the inorganic Br, that was later solubilised and determined by IC. In Fig. 4A, all the spectra showed a relatively pronounced peak depending on the DE reached, except in the case of the experiment 35 spectra (see Table S1) where a quasi-complete debromination was achieved. This confirmed that as expected, a high DE and highly solubilised Br were related to the absence of the C–Br stretching vibration of the TBBPA molecule in the residue. In the same way, Fig. 4B showed how only the two spectra related to the lowest DE achieved in those cases presented the peak. These two spectra could be differentiated from the other four, the spectra being different before and after the studied peak, because these were the residues of the 2 experiments in which MS was used instead of CaO 800 as a comparison with MS 800. However, the absence of a peak in experiment 6 (using CaO 800) compared to experiment 36 (using MS) was remarkable, since they had a similar DE. This could be due to the experimental error of approximately 4%. Experiment 6 had a DE close to 90%, whereas that of experiment 36 was approximately 80%.

The high amount of glass fibre present in the residues made Raman spectroscopy unfeasible because of the very high fluorescence coming from its Si–O bonds and from the resin phenolic parts. No signal of interest was detected, even when using a near-infrared laser.

3.2. *Preconditioning effect on the MCD process*

At this point of the study, the objective was to focus on the detected

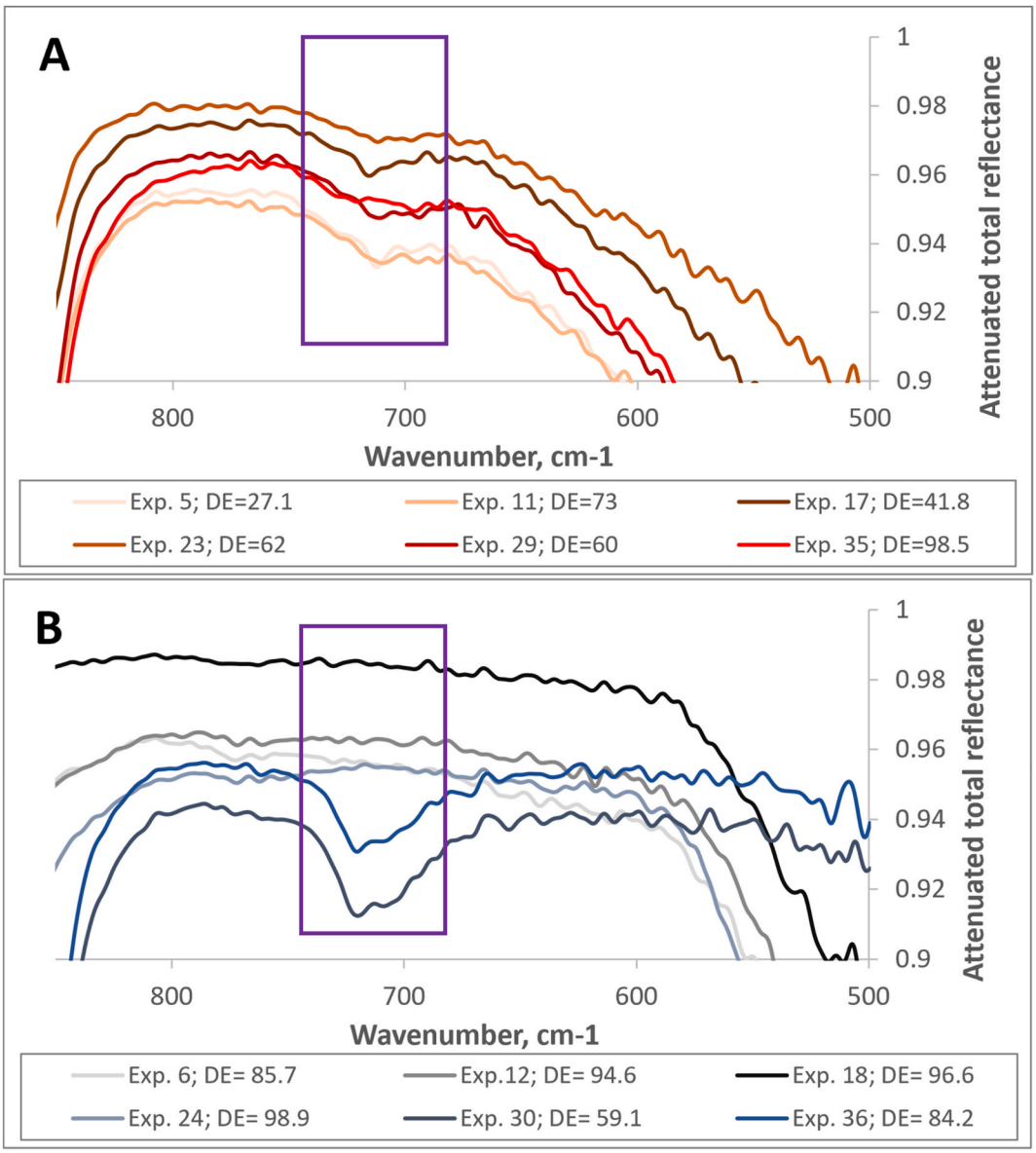

Fig. 4. Focused FTIR patterns of final residues using MS 800 (A) and CaO 800 or MS (B), with a purple framing denoting the peak band in the spectra coming from the C–Br stretching vibration of the TBBPA molecule. (For interpretation of the references to colour in this figure legend, the reader is referred to the Web version of this article.)

variables and parameters that had a great impact on the final debromination results, beyond the basic MCD parameters already considered. Those parameters were identified and included inside this study as a preconditioning, either by thermal treatment for precalcination, or by grinding/screening treatments, prior to MCD.

3.2.1. Effect of marble sludge precalcination and its characteristics

The three additives (CaO 800, MS and MS 800) were analysed by Raman spectroscopy and by TG in order to find which properties and/or characteristics could lead to the improvement of DE. Fig. 5 shows how the typical $Ca(OH)_2$ (around 356 and 3620 cm^{-1}) stretching vibrations were missing in the MS additive and clearly appeared in MS 800, as in the case of CaO 800. This would indicate a more reactive $Ca(OH)_2$ behaviour in the debromination reaction. Furthermore, several typical stretching vibrations of $CaCO_3$ (155, 282, 713 and 1086 cm^{-1}) present in both marble sludge samples were reduced by almost half, on average, for MS 800. This would indicate that $CaCO_3$ played a negligible role in the debromination.

In Fig. 6, 'w' was defined as the solid mass fraction and it represented the relationship between the total solid mass at any moment (m) with respect to the initial solid mass (m_0). Based on Ljupkovic (2013), the endothermic processes identified in Fig. 6 were a water evaporation at 100 °C, a $Ca(OH)_2$ dehydration at 400 °C, a $CaCO_3$ decomposition at 530–640 °C and a calcite ($CaCO_3$) decomposition at 730 °C.

Fig. 6A shows that the marble sludge calcination left a material with a TG curve that was more similar to that of calcined CaO (CaO 800), though with less pronounced weight losses at around 400 °C and 550 °C. In Fig. 6B, the DTGs help to better visualise those changes and the small weight losses at 550 °C of the calcined marble sludge are better appreciated. It seemed that the calcination of marble sludge at 850 °C for 2 h reduced the amount of $CaCO_3$ in the form of calcite (so calcination over a longer amount of time could reduce it even more) and produced more $Ca(OH)_2$ (already present in large quantities in calcined CaO, indicating that it could be the key to debromination). The original marble sludge (MS) had much more $CaCO_3$ in the form of calcite (because the sludge came from the cutting of the marble) than the calcined marble sludge

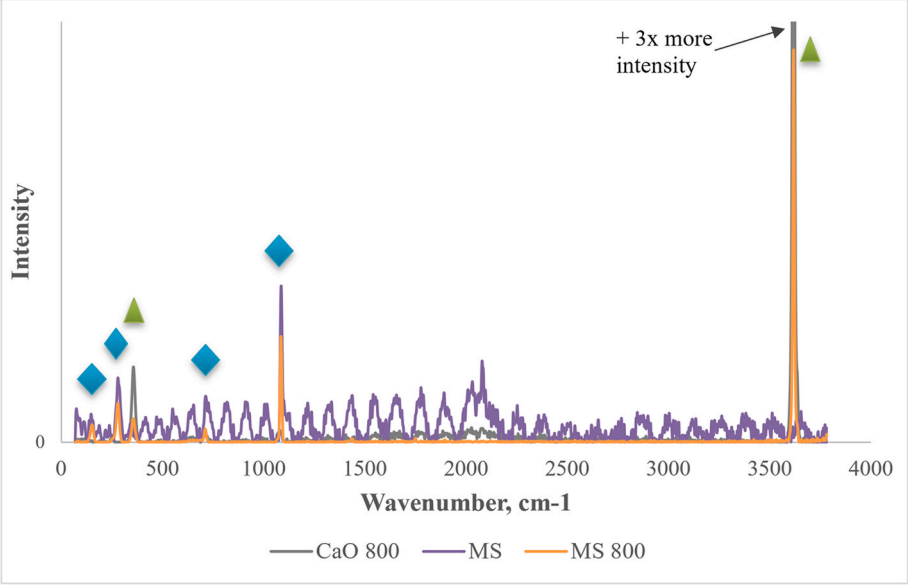

Fig. 5. Raman spectra of powders of CaO 800, MS and MS 800 samples with green triangles and blue rhombuses identifying the typical stretching vibrations of Ca $(OH)_2$ and $CaCO_3$, respectively (in agreement with the calcite spectra obtained by DOWNS (2006) and by Schmid and Dariz (2015). (For interpretation of the references to colour in this figure legend, the reader is referred to the Web version of this article.)

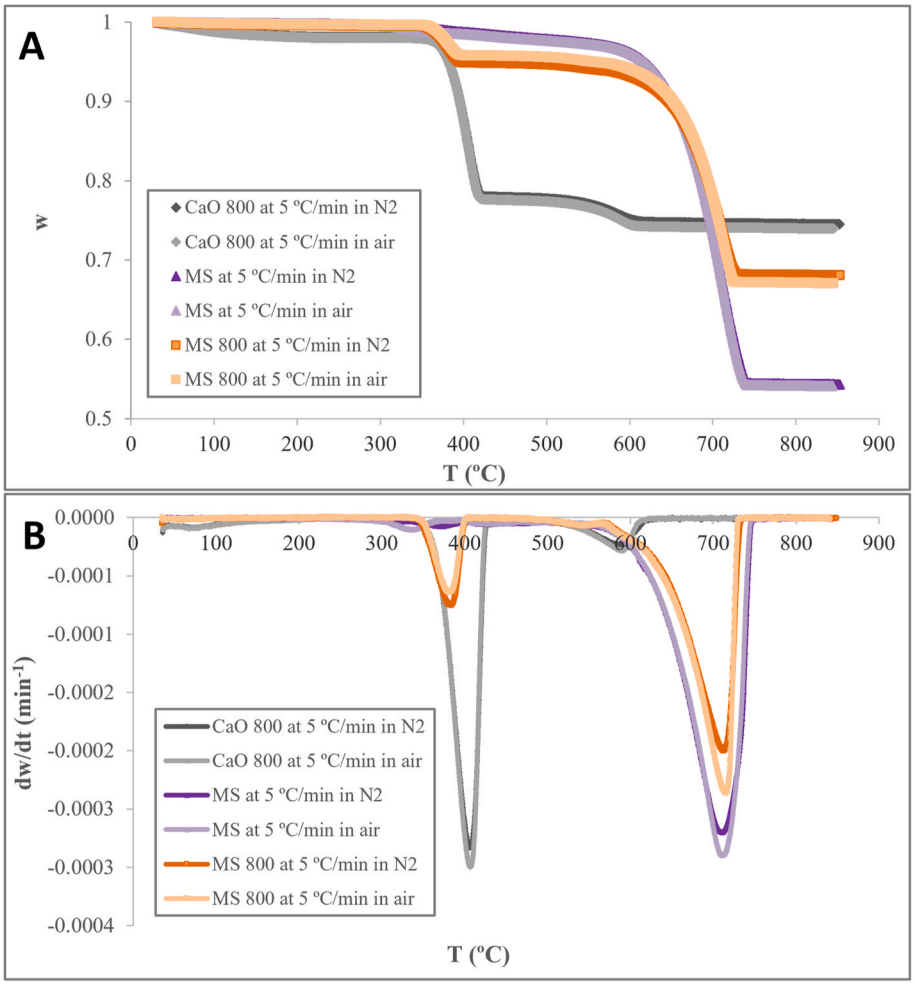

Fig. 6. (A). Thermal decompositions of the three additives employed (CaO 800, MS and MS 800), performed at 5 °C min^{-1} in air and N_2 (in order to indirectly confirm that no organics were present in these samples). (B). Differential thermogravimetric representations to facilitate the detection of small changes in the TGs concerned (the same colour was used for each related TG-DTG pair). . (For interpretation of the references to colour in this figure legend, the reader is referred to the Web version of this article.)

(MS 800), whose part of the present CaO was hydrated in the form of $Ca(OH)_2$.

A correspondence was noted between both analytical techniques employed. MS 800 showed a lower proportion of $CaCO_3$ and more $Ca(OH)_2$ than the original sludge, thus bearing a closer resemblance to the CaO 800 sample.

Schmid and Dariz (2015) showed that the Raman bands spotted during the analysis of pure CaO were due to inevitable traces of $Ca(OH)_2$ and $CaCO_3$, proving that CaO was a highly reactive material. In fact CaO reacts with H_2O very easily (it is very difficult not to find $Ca(OH)_2$ in a CaO sample) and $Ca(OH)_2$ is then easily carbonated with the CO_2 present in the air (this part could be effectively reduced by calcination) following the reversible chemical reaction equations shown below:

$$CaO + H_2O \leftrightarrow Ca(OH)_2 \quad (5)$$

$$Ca(OH)_2 + CO_2 \leftrightarrow CaCO_3 + H_2O \quad (6)$$

$CaCO_3$ was considered the least effective additive compared to CaO and a mixture of CaO and SiO_2. The performance of $Ca(OH)_2$ was also poorer than that of CaO (Saeki et al., 2001) but its formation is inevitable in a milling system with CaO (Zhang et al., 2010). In fact, although the CaO 800 sample was calcined for 2 h at 800 °C, Fig. 6 shows that the presence of $Ca(OH)_2$ was around 20% according to the weight loss at around 400 °C. In addition, this proportion had surely increased in the milling system in which H_2O was inevitably generated. This corroborates the fact that CaO reacts quickly with water present in the environment and that the CaO results were good, even in the presence of high levels of $Ca(OH)_2$. According to our results, the greater presence of $Ca(OH)_2$ compared to $CaCO_3$ clearly improved the debromination performance with respect to $CaCO_3$ (as calcite) only, hence the improvement in performance obtained with MS 800. This demonstrated that by extending calcination, it would be possible to further reduce the proportion of $CaCO_3$ and increase that of $Ca(OH)_2$ in order to improve the debromination effect by precalcination.

3.2.2. *Effect of sizing a WCB in accordance with the ball diameter*

Table S1 shows the details of the runs 25 to 36. They were performed to compare the importance of a correct WCB sizing selection with respect to the jar ball diameter/volume relationship applied, for mechanochemical debromination purposes. As noted in Fig. 3, contrary to what one would expect, the fact of increasing the WCB particle size improved the debromination, the debromination efficiency rising from around 60%–100%. This showed the importance of choosing the correct input size of the WCBs to be treated in accordance with the process parameters in use, particularly with the size of the balls with respect to the jar volume.

An increasing WCB input size usually creates more difficulties for the debromination reacting system. This was observed in a recent study by our research group on its effect during the hydrothermal treatment of large WCBs. Yet the latter should not apply in the case of mechanochemistry, however, where the effectiveness of the physical contact between reacting materials can be highly affected by huge reactant size differences. In fact, as already found by Xu et al. (2015), an optimal ball diameter exists during mechanochemical dechlorination for reductive degradation: larger balls present less space and a smaller impact area, inducing a process which may not provide enough energy. In addition, during the ball milling with CaO as additive, Zhang et al. (2012) found that pure TBBPA and CaO powder were becoming smaller and activated. However, long-term ball milling, the basis of WCB debromination, mainly acted with particles that were over a certain size and had little effect on the material particles, including PBDE-based WCBs, which are below this size (Wang et al., 2020). In fact the total energy transferred (D_0) (total energy effectively supplied to the powder being milled) was the only deciding factor of the conversion, with a certain ionic ratio (R) of a given additive, and once the additive was selected, DE only depended on D_0 and R (Chen et al., 2017). The results obtained in this work somewhat support those previous findings and corroborate the fact that to achieve a good D_0, it is important to consider an appropriate apparent ball diameter with respect to sample size.

In order to better support this, an empirically-based comparative model (already used in the recent study conducted by our group mentioned above) was applied. This model helped to understand the extent to which the global potential of the process was being exploited when seeking to adapt the WCB size to a given " ball diameter/jar volume" set, or to visualise the extent to which the potential of the available system was affected when overlooking this factor.

Table S3 shows a comparison of the debromination of different WCB particle sizes with both marble sludge versions. Those runs had identical experimental conditions and debromination agents, excepting the WCB size. The Total Surface of Contact (TSC) value was calculated as the sum of the surface area of all WCB particles that composed each reactant sample, assuming that these particles followed a quadrangular prismatic structure. In addition, a TSC ratio was calculated as the ratio between the Total Surface of Contact relating to powder (0.02 mm particles, according to the approximated final fineness obtained using a RETSCH RS 200 cryogenic mill) and larger WCB sizes of 0.84 mm. For these two WCBs sizes, 74,088 little quadrangular prismatic 0.02 mm particles fit inside a 0.84 mm quadrangular prismatic particle, and a calculated TSC ratio of 42 was obtained. This was expected to make the reaction much easier when using powder size WCB.

However, the situation was overturned when calculating the Impact on Debromination Efficiency due to Sample Size (IDESS) as the ratio between the debromination efficiencies obtained for powder and 0.84 mm WCB sizes during identical experimental conditions. Attending to these empirical comparative results, whether the sludge was calcined or not did not seem to influence the final result when considering the size of the WCB feeding the mill, and the impact that this would entail on the dehalogenation reaction. Even with a 42 times increase in the total TSC ratio, the debromination performance decreased on average by 36% (with a standard deviation of only around 3%) when reducing the WCB particle size. As previously mentioned, this finding was exactly the opposite of what has been established in other fields of dehalogenation treatments (Gandon-Ros et al., 2021b). To the best of our knowledge, this paper may be the first to report the influence of WCB size during its MCD. In fact, when reducing the size on an ongoing basis during milling, the reactants did not seem to continue to be activated as expected (which allowed them to react). This is because as the particles were already so small, they began to form aggregates between them, assisted by the presence of H_2O as a reaction product. This suggests the importance of reducing milling time when debrominating WCBs by ball milling (in addition to the time and energy involved) and of starting with larger size WCB, considering the ball mill feeding size limitations.

Therefore, although the benefits of marble sludge precalcination were not proven, there was no comparison with the great impact produced by a proper choice of WCB size according to the ball diameter/jar volume. And this was despite the great improvements that marble sludge calcination can bring to debromination, as illustrated in this work. This point deserves special attention in future works.

4. Conclusions

A complete debromination of 0.84 mm WCBs with TBBPA as brominated flame retardant (BFR) was achieved by MCT after only 10 h (more than 95% in only 5 h) when using precalcined marble sludge, another recoverable waste, as additive. Runs were performed at an intermediate rotation speed of 450 rpm, using additive/WCB mass ratios (R_m) of 8:1 and ball to powder ratios (BPR) of 50:1. The results suggest that the use of a lower R_m of 4:1 could positively influence debromination, allowing to obtain a complete or quasi-complete debromination within approximately the same amount of time while doubling the quantity of treated material by batch.

Marble sludge precalcination was also found necessary to meet this

objective, since it increased the proportion of $Ca(OH)_2$ through the decarbonation of $CaCO_3$ (as calcite), clearly improving final debromination performance.

Moreover, the results somewhat corroborate the fact that in order to achieve a desirable total of transferred energy from the milling balls to the material to debrominate, it is important to consider an appropriate apparent ball diameter (with respect to jar volume) in relation to WCB size.

In order to improve the viability of the process, it could be interesting in the future to undertake a more detailed study of marble sludge pre-calcination in view of maximising its effect on debromination performance. Another research line could focus on the optimisation and behaviour modelling of the WCB input size, once the specific parameters affected in the reaction system have been identified and set accordingly.

To conclude, this process has the ability to generate a debrominated WCB (after cleaning with water to solve the inorganic Br). On the one hand, this solid would be ready to be used as fuel for (co-) incineration processes such as cement kilns, where Ca and Mg from marble sludge and SiO_2 from fiberglass contained in the WCB would be beneficial. On the other, this final WCB could be recirculated again as a debrominating agent a number of times – to be determined – due to its high proportion of additive and SiO_2 (which would also act as a debromination facilitator).

CRediT authorship contribution statement

Gerard Gandon-Ros: Conceptualization, Methodology, Software, Validation, Formal analysis, Investigation, Resources, Data curation, Writing – original draft, Writing – review & editing, Visualization, Project administration. **Ignacio Aracil:** Writing – original draft, Writing – review & editing, Visualization. **María Francisca Gómez-Rico:** Writing – original draft, Writing – review & editing, Visualization. **Juan A. Conesa:** Writing – original draft, Supervision, Funding acquisition.

Declaration of competing interest

The authors declare that they have no known competing financial interests or personal relationships that could have appeared to influence the work reported in this paper.

Acknowledgements

This research was funded by the Ministry of Science and Innovation of Spain, grant numbers PID2019-105359RB-I00 (project) and BES-2017-080382 (scholarship). Support for this work was funded too by the University of Alicante, grant number UAUSTI20-05.

Appendix A. Supplementary data

Supplementary data to this article can be found online at https://doi.org/10.1016/j.jenvman.2022.115431.

References

Altarawneh, M., Dlugogorski, B.Z., 2015. Formation of polybrominated dibenzofurans from polybrominated biphenyls. Chemosphere 119, 1048–1053. https://doi.org/10.1016/j.chemosphere.2014.09.010.

Baláž, M., Baláž, P., Bujňáková, Z., Pap, Z., Kupka, D., Zorkovská, A., 2014. Mechanochemical dechlorination of PVC by utilizing eggshell waste. Acta Phys. Pol., A 126, 884–887. https://doi.org/10.12693/APHYSPOLA.126.884.

Cagnetta, G., Huang, J., Lu, M., Wang, B., Wang, Y., Deng, S., Yu, G., 2017. Defect engineered oxides for enhanced mechanochemical destruction of halogenated organic pollutants. Chemosphere 184, 879–883. https://doi.org/10.1016/j.chemosphere.2017.06.075.

Cagnetta, G., Robertson, J., Huang, J., Zhang, K., Yu, G., 2016. Mechanochemical destruction of halogenated organic pollutants: a critical review. J. Hazard Mater. 313, 85–102 https://doi.org/https://doi.org/10.1016/j.jhazmat.2016.03.076.

Chen, Z., Lu, S., Mao, Q., Buekens, A., Wang, Y., Yan, J., 2017. Energy transfer and kinetics in mechanochemistry. Environ. Sci. Pollut. Res. 24, 24562–24571. https://doi.org/10.1007/s11356-017-0028-9.

Composite Recycling Ltd, 2017. PCBRec Process: Waste Printed Circuit Board (WPCB) Recycling with Molten Salts. CORDIS EU Res. results.

Concas, A., Lai, N., Pisu, M., Cao, G., 2006. Modelling of comminution processes in spex mixer. Mill. Chem. Eng. Sci. 61, 3746–3760. https://doi.org/10.1016/j.ces.2006.01.007.

Dangtungee, R., Somchua, S., Siengchin, S., 2012. Recycling glass fiber/epoxy resin of waste printed circuit boards: morphology and mechanical properties. Mech. Compos. Mater. 48, 325–330. https://doi.org/10.1007/s11029-012-9279-1.

Dong, Y.Y., Li, Y., Zhao, C., Feng, Y., Chen, S., Dong, Y.Y., 2019. Mechanism of the rapid mechanochemical degradation of hexachlorobenzene with silicon carbide as an additive. J. Hazard Mater. 379, 120653.

Downs, R.T., 2006. The RRUFF project : an integrated study of the chemistry, crystallography, Raman and infrared spectroscopy of minerals. Progr. Abstr. 19th Gen. Meet. Int. Mineral. Assoc. Kobe, Japan 2006.

ECS Solid Biofuels - Determination of Ash Content, 2010. Solid Biofuels - Determination of Ash Content.

Eskenazi, B., Rauch, S.A., Tenerelli, R., Huen, K., Holland, N.T., Lustig, R.H., Kogut, K., Bradman, A., Sjödin, A., Harley, K.G., 2017. In utero and childhood DDT, DDE, PBDE and PCBs exposure and sex hormones in adolescent boys: the CHAMACOS study. Int. J. Hyg Environ. Health 220, 364–372. https://doi.org/10.1016/J.IJHEH.2016.11.001.

Forti, V., Balde, C.P., Kuehr, R., Bel, G., 2020. The Global E-Waste Monitor 2020: Quantities, Flows and the Circular Economy Potential. United Nations Univ. (UNU)/United Nations Inst. Train. Res. – Co-hosted SCYCLE Program. Int. Telecommun. Union Int. Solid Waste Assoc. (ISWA), pp. 1–119. Bonn/Geneva/Rotterdam.

Gandon-Ros, G., Nuñez, S.S., Ortuño, N., Aracil, I., Gómez-Rico, M.F., Conesa, J.A., 2021a. A win–win combination to inhibit persistent organic pollutant formation via the Co-incineration of polyvinyl chloride E-waste and sewage sludge. Polymers 13, 835. https://doi.org/10.3390/polym13050835.

Gandon-Ros, G., Soler, A., Aracil, I., Gómez-Rico, M.F., 2020. Dechlorination of polyvinyl chloride electric wires by hydrothermal treatment using K2CO3 in subcritical water. Waste Manag. 102, 204–211. https://doi.org/10.1016/j.wasman.2019.10.050.

Gandon-Ros, G., Soler, A., Aracil, I., Gómez-Rico, M.F., Conesa, J.A., 2021b. Improving efficiency and feasibility of subcritical water debromination of printed circuit boards E-waste via potassium carbonate adding. J. Clean. Prod. 319, 128605. https://doi.org/10.1016/j.jclepro.2021.128605.

Gilman, J.J., 1996. Mechanochemistry. Science 274, 65. https://doi.org/10.1126/SCIENCE.274.5284.65.

Guo, X., Xiang, D., Duan, G., Mou, P., 2010. A review of mechanochemistry applications in waste management. Waste Manag. 30, 4–10. https://doi.org/10.1016/J.WASMAN.2009.08.017.

Huang, A., Zhang, Z., Wang, N., Zhu, L., Z, J., 2016. Green mechanochemical oxidative decomposition of powdery decabromodiphenyl ether with persulfate. J. Hazard Mater. https://doi.org/doi: 10.1016/j.jhazmat.2015.09.072.

Leguen, R., 2019. Water Scarcity | Threats. WWF 1–5.

Lei, M., Wang, N., Guo, S., Zhu, L., Ding, Y., Tang, H., 2018. A one-pot consecutive photocatalytic reduction and oxidation system for complete debromination of tetrabromodiphenyl ether. Chem. Eng. J. 345, 586–593. https://doi.org/10.1016/J.CEJ.2018.01.143.

Ljupkovic, R.B., 2013. Reduction of Emission of Nitrogen and Carbon Oxides of Different Oxidation States by Using Biodiesel Produced over Cao Catalyst.

Moreno, A.I., Font, R., Gomez-Rico, M.F., 2019. Inhibition effect of polyurethane foam waste in dioxin formation. Waste Manag. 97, 19–26. https://doi.org/10.1016/j.wasman.2019.07.034.

Ren, Y., Kang, S., Zhu, J., 2015. Mechanochemical degradation of hexachlorobenzene using Mg/Al2O3 as additive. J. Mater. Cycles Waste Manag. 17, 607–615. https://doi.org/10.1007/s10163-015-0398-3.

Saeki, S., Kano, J., Saito, F., Shimme, K., Masuda, S., Inoue, T., 2001. Effect of additives on dechlorination of PVC by mechanochemical treatment. J. Mater. Cycles Waste Manag. 3, 20–23. https://doi.org/10.1007/s10163-000-0035-6.

Sakai, S., Watanabe, J., Honda, Y., Takatsuki, H., Aoki, I., Futamatsu, M., Shiozaki, K., 2001. Combustion of brominated flame retardants and behavior of its byproducts. Chemosphere 42, 519–531 https://doi.org/Doi: 10.1016/s0045-6535(00)00224-1.

Schmid, T., Dariz, P., 2015. Shedding light onto the spectra of lime: Raman and luminescence bands of CaO, Ca(OH)2 and CaCO3. J. Raman Spectrosc. 46, 141–146 https://doi.org/https://doi.org/10.1002/jrs.4622.

Schmidt, R., Martin Scholze, H., Stolle, A., 2016. Temperature progression in a mixer ball mill. Int. J. Ind. Chem. 72 7, 181–186. https://doi.org/10.1007/S40090-016-0078-8, 2016.

Soler, A., Conesa, J.A., Ortuño, N., 2017. Emissions of brominated compounds and polycyclic aromatic hydrocarbons during pyrolysis of E-waste debrominated in subcritical water. Chemosphere 186, 167–176. https://doi.org/10.1016/j.chemosphere.2017.07.146.

Song, J., Gao, X., Rong, Y., Zhang, D., Sui, H., 2019. Mechanism for degradation of dichlorodiphenyltrichloroethane by mechano-chemical ball milling with Fe-Zn bimetal. J. Environ. Manag. 247, 681–687. https://doi.org/10.1016/J.JENVMAN.2019.06.117.

Takacs, L., 2014. What is unique about mechanochemical reactions? Acta Phys. Pol., A 4, 1040–1043. https://doi.org/10.12693/APHYSPOLA.126.1040.

Tongamp, W., Zhang, Q., Shoko, M., Saito, F., 2009. Generation of hydrogen from polyvinyl chloride by milling and heating with CaO and Ni(OH)2. J. Hazard Mater. 167, 1002–1006. https://doi.org/10.1016/j.jhazmat.2009.01.076.

Wang, R., Zhu, Z., Tan, S., Guo, J., Xu, Z., 2020. Mechanochemical degradation of brominated flame retardants in waste printed circuit boards by Ball Milling. J. Hazard Mater. 385, 121509. https://doi.org/10.1016/J.JHAZMAT.2019.121509.

Xu, Z., Zhang, X., Fei, Q., 2015. Dechlorination of pentachlorophenol by grinding at low rotation speed in short time. Chin. J. Chem. Eng. 23, 578–582. https://doi.org/10.1016/j.cjche.2014.11.017.

Yi, Y., Kou, F., Tsang, P.E., Fang, Z., 2021. Highly efficient remediation of decabromodiphenyl ether-contaminated soil using mechanochemistry in the presence of additive and its mechanism. J. Environ. Manag. 299, 113595. https://doi.org/10.1016/J.JENVMAN.2021.113595.

Zhang, K., Huang, J., Zhang, W., Yu, Y., Deng, S., Yu, G., 2012. Mechanochemical degradation of tetrabromobisphenol A: performance, products and pathway. J. Hazard Mater. 243, 278–285. https://doi.org/10.1016/j.jhazmat.2012.10.034.

Zhang, Q., Saito, F., Ikoma, T., Shozo, T.-K., Kiyotaka, H., 2001. Effects of quartz addition on the mechanochemical dechlorination of chlorobiphenyl by using CaO. Environ. Sci. Technol. 35, 4933–4935. https://doi.org/10.1021/ES010638Q.

Zhang, Q., Saito, F., Shimme, K., Masuda, S., 1999. Dechlorination of PVC by a mechanochemical treatment under atmospheric condition. J. Soc. Powder Technol. Japan 36, 468–473. https://doi.org/10.4164/sptj.36.468.

Zhang, T., Huang, J., Zhang, W., Yu, Y., Deng, S., Wang, B., Yu, G., 2013. Coupling the dechlorination of aqueous 4-CP with the mechanochemical destruction of solid PCNB using Fe–Ni–SiO2. J. Hazard Mater. 250–251, 175–180. https://doi.org/10.1016/j.jhazmat.2013.01.072.

Zhang, W., Huang, J., Yu, G., Deng, S., Zhu, W., 2010. Mechanochemical destruction of Dechlorane Plus with calcium oxide. Chemosphere 81, 345–350. https://doi.org/10.1016/j.chemosphere.2010.07.025.